Microcomputed tomography analysis of particular autogenous bone graft in sinus augmentation at 5 months: differences on bone mineral density and 3D trabecular structure

Heng-Li Huang · Jui-Ting Hsu · Michael Y. C. Chen · Cheng Liu · Ching-Han Chang · Yu-Fen Li · Kuan-Ting Chen

Abstract

Objectives This study investigated the effects of gender on the three-dimensional (3D) bone mineral density (BMD) and micromorphology of the trabeculae of matured autogenous bone grafts after sinus floor augmentation, and compared them to those of adjacent native bone.

Materials and methods Ten bone biopsy samples were removed from the implant placement areas of patients who had received second-stage sinus floor augmentation, and analyzed by microcomputed tomography. BMD phantoms with two calcium hydroxyapatite densities (0.25 and 0.75 g/cm^3) were used to determine the BMD of the grafted and native bone samples. The 3D structural parameters of the trabeculae, including percentage of bone volume (bone volume/tissue volume, BV/TV), trabecular thickness (Tb.Th), trabecular number, trabecular separation, trabecular pattern factor (Tb.Pf), and structure model index, were analyzed between males and females and between grafted bone and native bone.

Results No significant gender-specific differences in BMD and 3D trabecular structure of either native or grafted bone were found ($P>0.05$). Compared to the adjacent native bone, the autogenous grafted bone exhibited lower BV/TV and Tb.Th as well as a higher Tb.Pf ($P<0.05$). Additionally, there was a weak positive correlation between the Tb.Th values of grafted and native bone ($R^2=0.58$).

Conclusions In the maxillary sinus, autogenous grafted bone exhibited lower BV/TV, Tb.Th, and trabecular connectivity than the adjacent native bone. No significant gender-specific differences were found for either the BMD or 3D trabecular structure of grafted bone.

Clinical relevance After bone remodeling, autogenous grafted bone revealed different 3D trabecular structure as compared to native bone.

H.-L. Huang (✉) · J.-T. Hsu · M. Y. C. Chen
School of Dentistry, China Medical University,
91 Hsueh-Shih Road,
40402, Taichung, Taiwan
e-mail: henleyh@gmail.com

C. Liu · C.-H. Chang
Institute of Biomedical Engineering,
National Cheng Kung University,
No. 1, University Road,
Tainan 701, Taiwan

C. Liu
Department of Plastic Surgery, Chi Mei Medical Center,
No. 901, Zhonghua Road,
Tainan 710, Taiwan

Y.-F. Li
Graduate Institute of Biostatistics, China Medical University,
91 Hsueh-Shih Road,
Taichung 404, Taiwan

Y.-F. Li · K.-T. Chen
Biostatistics Center, China Medical University,
91 Hsueh-Shih Road,
Taichung 404, Taiwan

Introduction

Oral rehabilitation of the atrophic edentulous posterior maxilla using dental implants is usually limited by the insufficient height of the alveolar bone. However, since Boyne and James first demonstrated the usefulness of autogenous grafts in the sinus floor [1], the grafting procedures that provide

the edentulous maxilla with various grafting materials are becoming increasingly important in implant treatment. In recent years, sinus floor augmentation has been a routine treatment that has resulted in favorable implant survival rates (<90 %) for 12–75 months [2].

Even though countless bone graft substitutes have been developed [3, 4], autogenous bone grafting remains the gold standard for sinus augmentation [2]. Autogenous bone grafting provides a satisfactory source of osteogenic cells without the risk of antigenicity [5]. Furthermore, due to its osteoconductive, osteoinductive, and osteogenic properties [6], autogenous bone is popular as a graft material for clinical use. Nevertheless, the volume of bone and the donor sites that can be harvested are limited. The iliac crest is a widely used donor site, as it has the greatest amount of available autogenous bone [3].

X-ray examination is a common method used to estimate clinically the condition of grafted bone. Although X-ray-based techniques are noninvasive, they provide only low-resolution, two-dimensional images. In contrast, microcomputed tomography (micro-CT) is a nondestructive procedure that provides quantitative and accurate evaluations of three-dimensional (3D) bone samples. Many studies have used micro-CT to evaluate the microlevel structure of the jaw bone [7–11] and the implant–bone interface [12, 13], and


Fig. 1 Photograph of a bone biopsy sample

confirmed its advantages, in particular for the in vitro assessment of the 3D bone structure.

Even though the technique of bone grafting has been increasingly employed in the clinical field, some reports still indicate that concerns regarding autogenous bone quality in elderly patients and postmenopausal women have limited the use of autogenous bone grafting [14, 15]. Micro-CT has been used as a tool to investigate the 3D architecture of grafted bone [16–19], and it seems a practical method for investigating the gender differences (if any) in bone mineral density (BMD) and 3D trabecular architecture

Fig. 2 The micro-CT images of the native bone (**a**), grafted bone (**b**), native bone with region of interest (ROI) (**c**), and grafted bone with ROI (**d**)
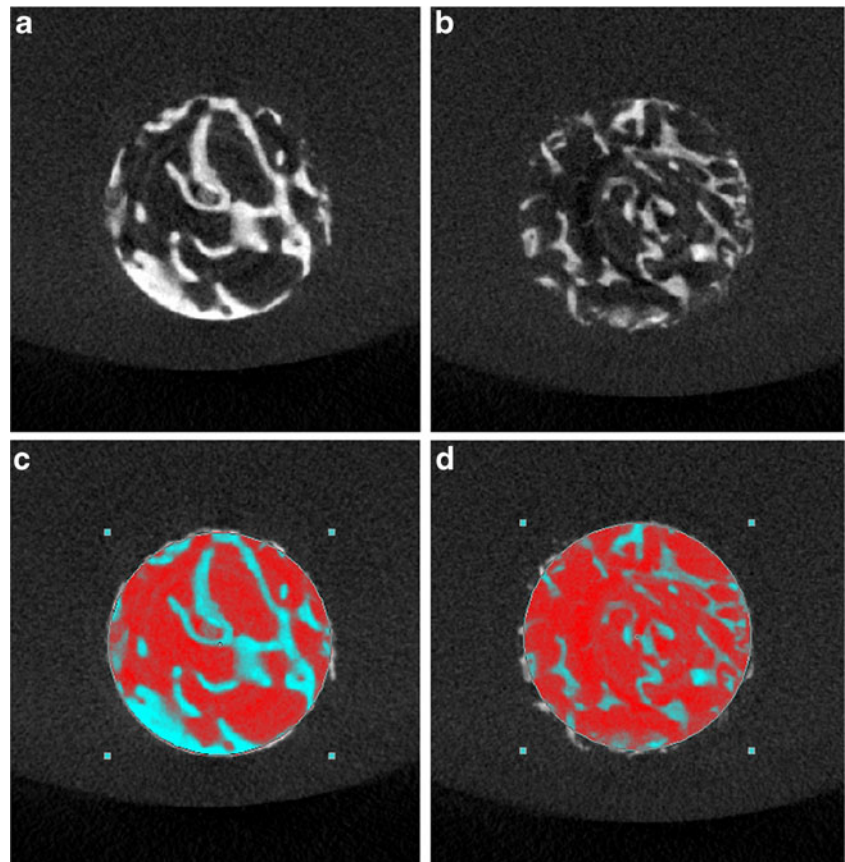
of grafted bone, especially for older patients. This study also examined the differences of BMD and 3D trabecular structure between the matured autogenous bone graft and the adjacent native bone.

Materials and methods

Bone biopsy preparation

Six men and four women aged 44–58 years had undergone the surgery of sinus floor augmentation with autogenous bone grafts because of insufficient height of the alveolar bone to allow dental implant placement. None of the patients had systemic pathologies affecting immune system functioning, non-insulin-dependent diabetes mellitus, or previous history of drug abuse. After being informed about the procedure, all of the patients gave written informed consent to participate in the study. The study protocol was approved by the Institutional Committee of China Medical University Hospital, Taichung, Taiwan (DMR96-IRB-180 & DMR97-IRB-260). After a 4- to 5-month healing period for maturation of autogenous bone graft, ten rod-shaped bone samples containing the native and grafted region of bone tissue were retrieved by trephine osteotomy (4.0 mm inner diameter) from the grafted site during surgical reentry for dental implant placement (Fig. 1). After receiving the biopsy specimens of bone tissue, the specimens were placed immediately in 10 % neutral buffered formalin solution.

Micro-CT scanning

The samples were scanned with a high-resolution cone beam micro-CT system (SkyScan 1076; SkyScan, Aartselaar, Belgium) to quantify the BMD (in grams per cubic centimeter) and other parameters related to 3D microarchitectures of trabecular bone. Before scanning, the bone biopsy samples were rinsed and stored in physiological saline solution (0.9 %) within a polypropylene tube. The X-ray source was set at 49 kV and 200 μA with the aid of a 0.5-mm-thick aluminum filter to optimize the contrast, a 360° rotation, a rotation step of 0.4° (2,700 images per scan), three-frame averaging, and an exposure time of 1,180 ms. The image resolution was fixed at a voxel size of 17.2 μm. During scanning, two BMD phantoms (SkyScan) that were 4.0 mm in diameter, 5.5 mm long, and had calcium hydroxyapatite densities of 0.25 and 0.75 g/cm^3 were placed near the bone biopsy samples to aid BMD calculation.

NRecon reconstruction software (NRecon v.1.4.4, SkyScan) was used to create two-dimensional, 1,000× 1,000-pixel images. For the reconstruction parameters, ring artifact correction and smoothing were fixed at zero, and the

beam hardening correction was set at 0 %. Contrast limits were applied following SkyScan instructions. The lower limit was zero so that the density scale had a zero origin. The upper limit was at the top end of the brightness spectrum, representing the highest bone density value. The quantification of native and grafted bone requires analyzing a similar volume of interest (VOI) in each 3D image. Since the bone sample is a rod-shaped specimen with 4 mm diameter, the selected VOI was also rod shaped with the same diameter for both BMD and trabecular structure calculations. The reconstructed images of water within the selected VOI were used to calibrate the standard unit of X-
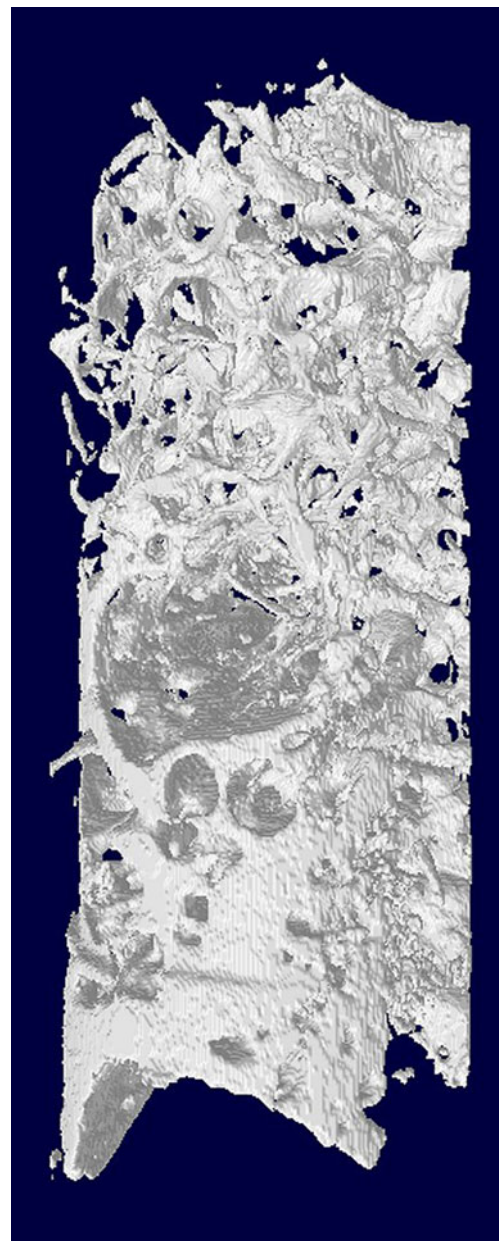

Fig. 3 Micro-CT 3D reconstruction of a bone biopsy sample containing the VOIs of native bone (*lower part*) and grafted bone (*upper part*)

ray computed tomography density (Hounsfield unit, HU) by using MicroCT analyzer software (CTAn; v.1.6.0, SkyScan) provided by SkyScan. A similar procedure was used to measure the HU values of two BMD phantom rods, followed by conversion from HU to BMD values (in grams per cubic centimeter). Once the calibration of BMD against HU values was complete, the same VOI was applied to the images of the bone biopsy samples (Fig. 2) to calculate the BMD values of the grafted and native bone. All the BMD calculations were executed by CTAn software. The 3D structure of bone biopsy (Fig. 3) was also analyzed for grafted bone and native bone individually by CTAn. In order to distinguish grafted bone or native bone from the background which consists of saline solution, a suitable threshold range is required. Since a wide threshold range makes the trabeculae too thick whereas a narrow threshold tends to disconnect thinner trabeculae, the bone segmentation threshold range was set between 110 and 255 (in gray values; Fig. 4) for both grafted bone and native bone in the analysis of 3D trabecular characteristics. The analyzed parameters of 3D trabecular structure included the percentage of bone volume [bone volume/tissue volume (BV/TV), in percent], trabecular thickness (Tb.Th, pixels), trabecular number (Tb.N, 1/pixel), trabecular separation (Tb.Sp, pixels), trabecular pattern factor (Tb.Pf, 1/pixel), and the structure model index (SMI). BV/TV represents the percentage of BV relative to TV within a VOI. Tb.Th indicates the mean thickness of individual trabecular bones within a VOI. Tb.N signifies the number of traversals across a trabecular bone per unit length on a linear path within a VOI. Tb.Sp represents the relative spacing between individual trabecular bones within a VOI. Tb.Pf was developed by Hahn et al. in 1992 [20] and a lower Tb.Pf signifies better connected trabecular lattices, while a higher Tb.Pf indicates a more disconnected trabecular structure. SMI was derived according to the method of

Hildebrand and Ruegsegger in 1997 [21]. SMI is used to characterize trabecular bone according to its transition from plate-like to rod-like architecture. An ideal plate and cylinder have SMI values of 0 and 3, respectively.

Statistical and correlation analyses

All of the micro-CT measurement parameters are summarized as mean and standard deviation values. Paired t test was used for the comparison between grafted bone and native bone. Comparisons of the parameters between male and female were analyzed with Student's t test. For the significant results ($P \leq 0.05$) of parameters between native bone and grafted bone, the linear regression models were also performed and the goodness of fit for regression models was qualified using R^2 values. All of the statistical analyses were executed using SAS software (SAS v9.2; SAS Institute, Cary, NC, USA). The level of statistical significance was set at $\alpha = 0.05$.

Results

The micro-CT findings (including those of the BMD and 3D trabecular structure) of grafted bone and the adjacent native bone are summarized in Table 1. The mean and standard deviation values of all of the measured parameters for both the grafted and native bone are listed in Table 2. Significant differences between the two bone types were observed for only three parameters: BV/TV, Tb.Th, and Tb.Pf ($P<0.05$). BV/TV and Tb.Th were 35.5 and 37.7 % greater for native bone than for grafted bone, respectively, while Tb.Pf was lower for native bone [0.07 (1/pixel)] than for grafted bone [0.19 (1/pixel)]. Since significant outcomes were found for only BV/TV, Tb.Th, and Tb.Pf ($P<0.05$), correlations of BV/TV, Tb.Th, and Tb.Pf between the grafted and native bone are shown in

Fig. 4 The original micro-CT image of grafted bone containing the gray values between 0 and 255 (a). A fixed threshold range between 110 and 255 was applied to the image of grafted bone (b) for the segmentation of bone from the background
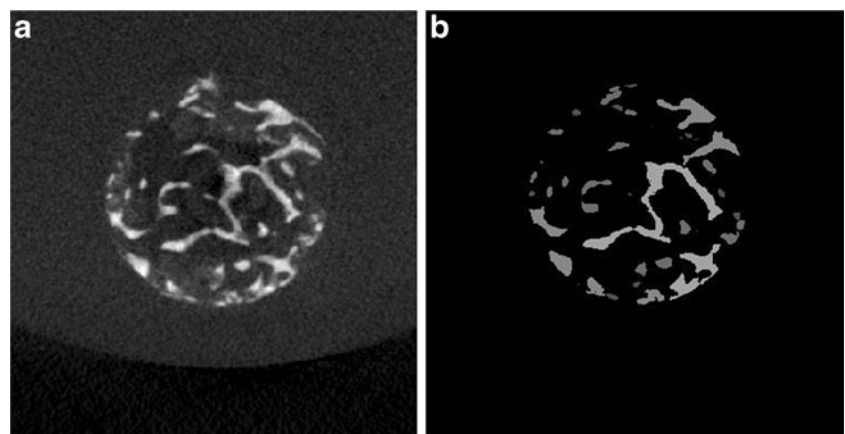
Table 1 The quantitative data of micro-CT measurement parameters of (autogenous) grafted bone and native bone by micro-CT analysis (1 pixel=17.2 μm)

No.	Sex, age (years)		BMD (g/cm^3)	BV/TV (%)	Tb.Th (pixel)	Tb.N (1/pixel)	Tb.Sp (pixel)	Tb.Pf (1/pixel)	SMI (none)
1	Female, 44	N	0.090	16.54	10.12	0.016	39.85	0.094	1.87
		G	0.031	8.74	6.48	0.014	25.12	0.257	2.45
2	Male, 58	N	0.080	18.65	8.87	0.021	29.35	0.117	1.84
		G	0.075	15.43	7.85	0.020	25.61	0.167	2.14
3	Male, 49	N	0.295	30.31	13.71	0.022	29.31	0.072	1.69
		G	0.099	12.64	7.79	0.016	26.74	0.213	2.41
4	Female, 49	N	0.330	34.35	12.53	0.027	24.22	0.047	1.67
		G	0.372	41.11	10.59	0.039	17.25	0.032	1.28
5	Male, 48	N	0.764	24.44	13.71	0.018	34.85	0.036	1.80
		G	0.391	19.43	8.45	0.023	17.41	0.146	2.43
6	Male, 50	N	0.216	20.05	11.05	0.018	35.01	0.024	1.38
		G	0.020	1.85	4.85	0.004	36.73	0.496	2.82
7	Female, 49	N	0.028	15.31	10.88	0.014	37.04	0.112	2.26
		G	0.119	27.89	9.16	0.030	20.62	0.053	1.66
8	Male, 53	N	0.084	46.43	19.32	0.024	28.59	0.017	1.40
		G	0.341	15.43	7.46	0.021	27.74	0.202	2.21
9	Male, 53	N	0.444	75.09	25.66	0.029	17.50	0.091	1.54
		G	0.300	49.50	16.47	0.030	20.76	0.035	0.82
10	Female, 61	N	0.448	45.79	18.90	0.024	23.29	0.083	2.39
		G	0.158	15.32	11.05	0.014	27.99	0.260	2.39

N native bone, *G* grafted bone

Fig. 5. A weakly positive correlation was found between the Tb.Th values of grafted and native bone ($R^2=0.58$), while no apparent correlation was found for BV/TV ($R^2=0.31$) and Tb.Pf ($R^2=0.15$) between the two bone types.

Table 3 details the differences in trabecular BMD and 3D architecture in grafted bone and the adjacent native bone between males and females. With the exception of SMI in native bone, there were no significant gender-specific differences in either BMD or 3D trabecular structure for the two bone types ($P>0.05$).

Table 2 The mean (standard deviation) data of micro-CT BMD and 3D structural parameters of native bone and grafted bone

Variable	Native bone ($n=10$)	Grafted bone ($n=10$)	P value
BMD (g/cm^3)	0.28 (0.23)	0.19 (0.15)	0.180
BV/TV (%)	32.69 (18.72)	21.07 (14.26)	0.037
Tb.Th (pixel)	14.48 (5.25)	9.02 (3.19)	0.001
Tb.N (1/pixel)	0.02 (0.00)	0.02 (0.01)	0.885
Tb.Pf (1/pixel)	0.07 (0.04)	0.19 (0.14)	0.042
SMI (none)	1.78 (0.33)	2.06 (0.62)	0.236
Tb.Sp (pixel)	29.90 (6.93)	24.60 (5.88)	0.073

Mean (standard deviation), compared by paired *t* test

Discussion

Intraoral radiology is noninvasive, low cost, readily available, well tolerated by patients, and user-friendly [22], and as such, it has been widely used to estimate the bone quality of grafted sites prior to dental implant placement. Even though intraoral radiography is popular in clinics, it provides only low-resolution and two-dimensional images, which limits the visibility of the sites of interest. Histology and histomorphometric techniques can be used to examine the bone mineral quality and trabecular bone structure of grafted bone, but they can only provide one-time measurements that cannot be repeated on the same sample [23]. Nowadays, new imaging techniques such as cone beam computed tomography and micro-CT have made it possible to obtain high-resolution 3D images, and micro-CT has further provided the ability to directly analyze the bone architecture. However, until now, 3D BMD measurement and trabecular structure estimation on micro-CT have not been well investigated for autogenous bone graft in sinus augmentation. The present study used micro-CT accompanied by 3D medical image processing to reconstruct and measure the precise 3D BMD and bone architecture of autogenous grafted bone; the obtained data would be particularly useful in maxillary sinus floor augmentation.

Fig. 5 Linear regressions and squared correlation coefficients of BV/TV (**a**), Tb.Th (**b**), and Tb.Pf (**c**) between native bone and grafted bone
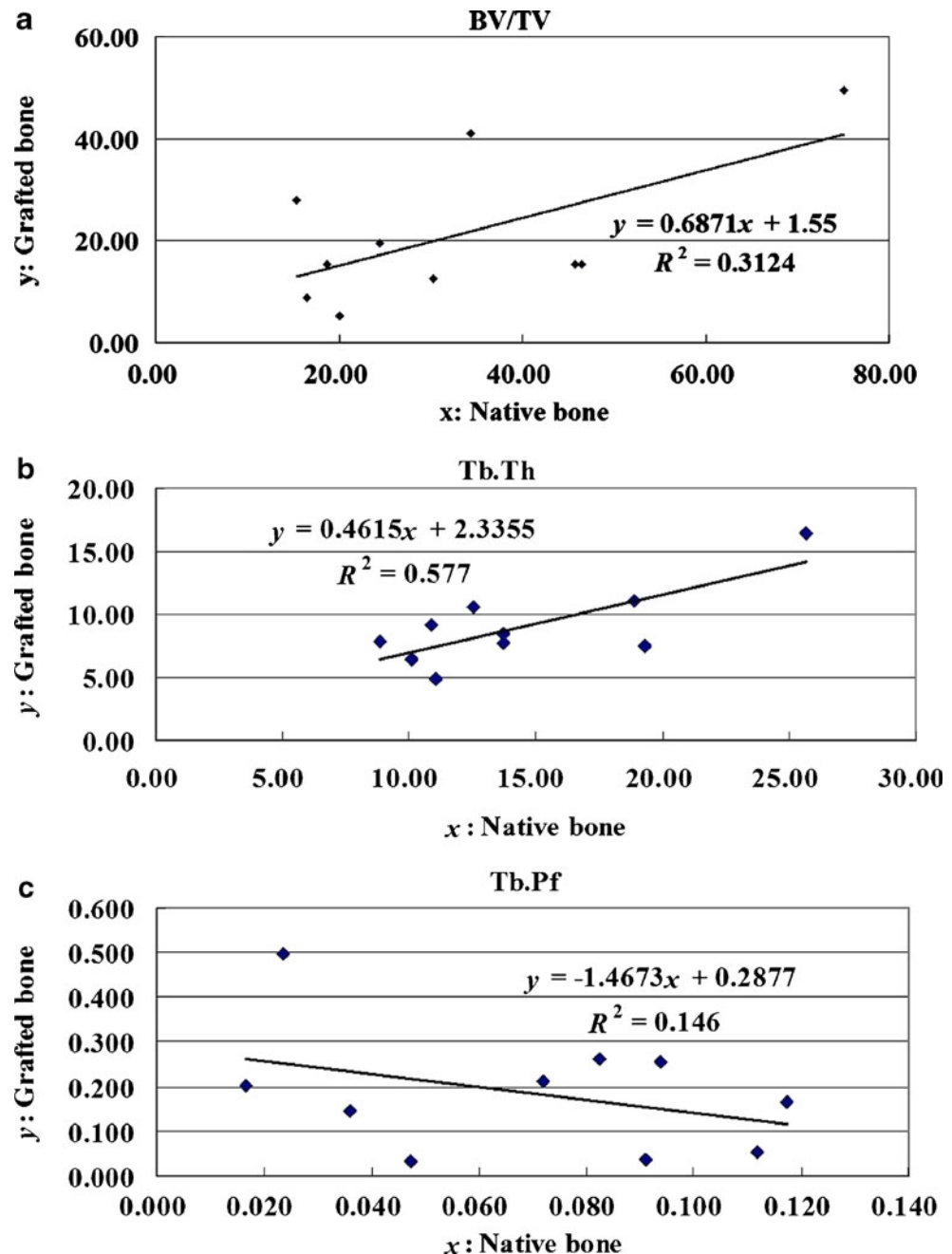
With regard to the outcomes of BMD and 3D structural parameters of trabecular bone between native and matured grafted bone (Table 2), we found that not only the percentage of bone volume but some of the trabecular morphologies differed between grafted and native bone. BV/TV and Tb.Th were significantly lower, and Tb.Pf was significantly higher in the grafted bone than in the native bone. This makes sense for the grafted bone because the thinness of trabeculae not only diminishes the bone volume but also makes the trabecular bone more disconnected (a higher Tb.Pf indicates a more disconnected trabecular structure). The relationships of BV/TV, Tb.Th, and Tb.Pf between grafted and native bone were also evaluated. A weakly positive correlation was found for Tb.Th between grafted and native bone, but no correlation was found for BV.TV and Tb.Pf. This implies that the condition of native bone in the atrophic maxilla is unlikely to influence the condition of the adjacent grafted bone.

Since BV/TV, Tb.Th, and Tb.Pf are indexes that reflect the volume of trabecular bone as well as the status of the trabecular structure. These results revealed that the volume, thickness, and connectivity of trabeculae were both lower in the grafted bone than in the native bone from the atrophic

Table 3 *P* values of BMD and 3D structure parameters between male and female

Bone type	Variable	Male (*n*=6)	Female (*n*=4)	*P* value
Native bone	Age (years)	51.83 (3.66)	50.75 (7.23)	0.759
	BMD (g/cm^3)	0.31 (0.26)	0.22 (0.20)	0.576
	BV/TV (%)	35.83 (21.72)	28.00 (14.71)	0.549
	Tb.Th (pixel)	15.39 (6.13)	13.11 (3.99)	0.534
	Tb.N (1/pixel)	0.02 (0.00)	0.02 (0.01)	0.652
	Tb.Pf (1/pixel)	0.06 (0.04)	0.08 (0.03)	0.325
	SMI (none)	1.61 (0.20)	2.05 (0.33)	0.030
	Tb.Sp (pixel)	29.10 (6.37)	31.10 (8.57)	0.681
Grafted bone	BMD (g/cm^3)	0.20 (0.16)	0.17 (0.14)	0.737
	BV/TV (%)	19.61 (15.39)	23.27 (14.31)	0.715
	Tb.Th (pixel)	8.81 (3.96)	9.32 (2.06)	0.822
	Tb.N (1/pixel)	0.02 (0.01)	0.02 (0.01)	0.453
	Tb.Pf (1/pixel)	0.21 (0.15)	0.15 (0.13)	0.539
	SMI (none)	2.14 (0.69)	1.95 (0.57)	0.655
	Tb.Sp (pixel)	25.83 (6.63)	22.75 (4.76)	0.449

Mean (standard deviation), compared by Student's *t* test

maxilla; caution is necessary when applying immediate loading of the implant following sinus floor augmentation. Although immediate loading treatment has been reported to be a reliable surgical procedure in edentulous maxillae [24], the lower stiffness of the grafted bone in the sinus may increase the stress levels in the alveolar ridge around the implant [25].

The results of this study revealed no significant difference in 3D BMD between men and women for grafted bone. This finding is similar to some studies in which differences in the bone density and bone quantities of grafted bone between males and females were evaluated by two-dimensional histomorphometric or microradiographic evaluations [26, 27]. These studies showed no significant gender-specific differences in the outcome. In addition, the present study also showed that the 3D trabecular structure of grafted bone is not affected by gender. Therefore, gender-specific associations may not the major factor to influence either bone density (BMD) or bone quality (morphology of trabeculae) of grafted bone. For native bone, this study also exhibited no apparent difference in BMD. This outcome is consistent with the finding of Shapurian et al. [28] which indicated no relationship between the bone density (in Hounsfield units) and gender by using 3D assessment of CT images. Nevertheless, the results of this study did not signify that gender is not a factor to affect the native bone density. The incidence of bone loss in the elder population is dependent on gender [29]. The older postmenopausal women are considered to expose to the highest risk of osteoporosis [30].

One of the limitations of this study is the location of the donor site. Even though cancellous iliac bone was the main autogenous graft material used in the patients in this study, as suggested by Gerressen et al. [26, 31], further clinical studies are needed to elucidate the detailed mechanisms underlying the effect of various donor sites on the BMD and 3D trabecular structure of matured grafted bone in the maxillary sinus. Another limitation is the small sample. Although our patient evaluation was objective, and the patients were carefully assessed to ensure that they did not have any physiological disease, a larger sample is required to strengthen the statistical power of the findings. However, we do believe that the present findings are worthwhile, and can be regarded as being generally applicable and thus useful to clinicians.

Conclusions

The following conclusions can be drawn from the findings of this study:

1. BV/TV, Tb.Th, and the connectivity of the trabeculae (i.e., Tb.Pf) are both lower in grafted than native bone. There is a weak positive correlation in Tb.Th values between native bone and grafted bone.
2. The BMDs and 3D trabecular structures of native bone and grafted bone do not differ significantly with gender.

References

1. Boyne P, James R (1980) Grafting of the maxillary sinus floor with autogenous marrow and bone. J Oral Surg 38:613–616
2. Del Fabbro M, Testori T, Francetti L, Weinstein R (2004) Systematic review of survival rates for implants placed in the grafted maxillary sinus. Int J Periodontics Restorative Dent 24:565–577
3. Garg AK (2004) Bone biology, harvesting, and grafting for dental implants: rationale and clinical applications. In: Garg AK (ed) Review of bone-grafting materials, 1st edn. Quintessence Publishing Co., Carol Steam, pp 23–24
4. Scarano A, Degidi M, Iezzi G, Pecora G, Piattelli M, Orsini G, Caputi S, Perrotti V, Mangano C, Piattelli A (2006) Maxillary sinus augmentation with different biomaterials: a comparative histologic and histomorphometric study in man. Implant Dent 15:197–207
5. Kaufman E (2003) Maxillary sinus elevation surgery: an overview. J Esthet Restor Dent 15:272–283

6. Nkenke E, Stelzle F (2009) Clinical outcomes of sinus floor augmentation for implant placement using autogenous bone or bone substitutes: a systematic review. Clin Oral Implants Res 20:124–133

7. Fanuscu M, Chang T (2004) Three dimensional morphometric analysis of human cadaver bone: microstructural data from maxilla and mandible. Clin Oral Implants Res 15:213–218

8. Stoppie N, Pattijn V, Cleynenbreugel T, Wevers M, Sloten JV, Ignace N (2006) Structural and radiological parameters for the characterization of jawbone. Clin Oral Implants Res 17:124–133

9. Nampo T, Watahiki J, Enomoto A, Taguchi T, Ono M, Nakano H, Yamamoto G, Irie T, Tachikawa T, Maki K (2010) A new method for alveolar bone repair using extracted teeth for the graft material. J Periodontol 81:1264–1272

10. Muhlberger G, Svejda M, Lottersberger C, Emshoff R, Putz R, Kuhn V (2009) Mineralization density and apparent density in mandibular condyle bone. Oral Surg Oral Med Oral Pathol Oral Radiol Endod 107:573–579

11. Rebaudi A, Benedicenti S (2010) Sinus grafting with magnesium-enriched bioceramic granules and autogenous bone: a microcomputed tomographic evaluation of 11 patients. Int J Periodontics Restorative Dent 30:53–61

12. Morinaga K, Kido H, Sato A, Watazu A, Matsuura M (2009) Chronological changes in the ultrastructure of titanium bone interfaces: analysis by light microscopy, transmission electron microscopy, and micro computed tomography. Clin Implant Dent Relat Res 11:59–68

13. Ohashi T, Matsunaga S, Nakahara K, Abe S, Ide Y, Tamatsu Y, Takano N (2010) Biomechanical role of peri-implant trabecular structures during vertical loading. Clin Oral Invest 14:507–513

14. Muschler GF, Nitto H, Boehm CA, Easley KA (2001) Age and gender related changes in the cellularity of human bone marrow and the prevalence of osteoblastic progenitors. J Orthop Res 19:117–125

15. Gamradt SC, Lieberman JR (2003) Bone graft for revision hip arthroplasty: biology and future applications. Clin Orthop Relat Res 417:183–194

16. Trisi P, Rebaudi A, Calvari F, Lazzara R (2006) Sinus graft with biogran, autogenous bone, and PRP: a report of three cases with histology and micro-CT. Int J Periodontics Restorative Dent 26:113–125

17. Chopra P, Johnson M, Nagy T, Lemons J (2009) Micro computed tomographic analysis of bone healing subsequent to graft placement. J Biomed Mater Res B Appl Biomater 88:611–618

18. Kon K, Shiota M, Ozeki M, Yamashita Y, Kasugai S (2009) Bone augmentation ability of autogenous bone graft particles with different sizes: a histological and micro computed tomography study. Clin Oral Implants Res 20:1240–1246

19. Kuhl S, Gotz H, Hansen T, Behneke A, Heil U, Duschner H, d'Hoedt B (2010) Three-dimensional analysis of bone formation after maxillary sinus augmentation by means of microcomputed tomography: a pilot study. Int J Oral Maxillofac Implants 25:930–938

20. Hahn M, Vogel M, Pompesius-Kempa M, Delling G (1992) Trabecular bone pattern factor—a new parameter for simple quantification of bone microarchitecture. Bone 13:327–330

21. Hildebrand T, Ruegsegger P (1997) Quantification of bone microarchitecture with the structure model index. Comput Methods Biomech Biomed Eng 1:15–23

22. Dos Santos CL, Jacobs R, Quirynen M, Huang Y, Naert I, Duyck J (2011) Peri-implant bone tissue assessment by comparing the outcome of intra oral radiograph and cone beam computed tomography analyses to the histological standard. Clin Oral Implants Res 22:492–499

23. Gedrange T, Hietschold V, Mai R, Wolf P, Nicklisch M, Harzer W (2005) An evaluation of resonance frequency analysis for the determination of the primary stability of orthodontic palatal implants. A study in human cadavers. Clin Oral Implants Res 16:425–431

24. Degidi M, Piattelli A, Felice P, Carinci F (2005) Immediate functional loading of edentulous maxilla: a 5-year retrospective study of 388 titanium implants. J Periodontol 76:1016–1024

25. Huang HL, Fuh LJ, Hsu JT, Tu MG, Shen YW, Wu CL (2008) Effects of implant surface roughness and stiffness of grafted bone on an immediately loaded maxillary implant: a 3D numerical analysis. J Oral Rehabil 35:283–290

26. Gerressen M, Hermanns Sachweh B, Riediger D, Hilgers RD, Spiekermann H, Ghassemi A (2009) Purely cancellous vs. cortico-cancellous bone in sinus floor augmentation with autogenous iliac crest: a prospective clinical trial. Clin Oral Implants Res 20:109–115

27. Schlegel KA, Schultze Mosgau S, Wiltfang J, Neukam FW, Rupprecht S, Thorwarth M (2006) Changes of mineralization of free autogenous bone grafts used for sinus floor elevation. Clin Oral Implants Res 17:673–678

28. Shapurian T, Damoulis PD, Reiser GM, Griffin TJ, Rand WM (2006) Quantitative evaluation of bone density using the Hounsfield index. Int J Oral Maxillofac Implants 21:290–297

29. Thomsen K, Gotfredsen A, Christiansen C (1986) Is postmenopausal bone loss an age-related phenomenon? Calcif Tissue Int 39:123–127

30. von Wowern N (2001) General and oral aspects of osteoporosis: a review. Clin Oral Invest 5:71–82

31. Gerressen M, Prescher A, Riediger D, Van Der Ven D, Ghassemi A (2008) Tibial versus iliac bone grafts: a comparative examination in 15 freshly preserved adult cadavers. Clin Oral Implants Res 19:1270–1275